Journal of Geosciences, 60 (2015), 113–121 DOI: 10.3190/jgeosci.192

Original paper

Svornostite, $K_2Mg[(UO_2)(SO_4)_2]_2 \cdot 8H_2O$, a new uranyl sulfate mineral from Jáchymov, Czech Republic

Jakub PLÁŠIL[1*], Jan HLOUŠEK[2,†], Anatoly V. KASATKIN[3], Milan NOVÁK[4], Jiří ČEJKA[5], Ladislav LAPČÁK[6]

[1] *Institute of Physics, Academy of Sciences of the Czech Republic v.v.i., Na Slovance 2, 182 21 Prague 8, Czech Republic; plasil@fzu.cz*
[2] *U Roháčových kasáren 24, 100 00 Prague 10, Czech Republic*
[3] *Fersman Mineralogical Museum of the Russian Academy of Sciences, Leninsky Prospekt 18-2, 119071 Moscow, Russia*
[4] *Department of Geological Sciences, Masaryk University, Kotlářská 2, 611 37 Brno, Czech Republic*
[5] *Department of Mineralogy and Petrology, National Museum, Cirkusová 1740, 193 00 Prague 9, Czech Republic*
[6] *Institute of Chemical Technology, Prague, Technická 5, 166 28 Prague 6, Czech Republic*
[†] *deceased on April 27, 2014*
**Corresponding author*

Svornostite (IMA2014-078), $K_2Mg[(UO_2)(SO_4)_2]_2 \cdot 8H_2O$, is a new uranyl sulfate mineral from Jáchymov, Western Bohemia, Czech Republic. The new mineral was found in material originating from the Geschieber vein in the Svornost mine. It occurs as crystalline crusts composed of yellow prismatic crystals on a gangue along with geschieberite, adolfpateraite and gypsum. It is a low-temperature, supergene mineral formed by the post-mining weathering of uraninite. Svornostite is orthorhombic, the space group $Pmn2_1$, with the unit-cell parameters a = 12.7850(3), b = 8.2683(4), c = 11.2163(3) Å, V= 1185.68(7) Å^3 and Z = 2. Crystals are long prisms elongated on [001] and flattened on {100}. Crystals exhibit the forms {100}, {010} and {011}, usually forming multiple intergrowths. Svornostite is light yellow and has a very pale yellow streak. It exhibits a strong yellowish-green fluorescence under both long-wave and short-wave UV. It is translucent to transparent with strong vitreous luster. The mineral has a Mohs hardness ~2; it is brittle, with uneven fracture and a perfect cleavage, on {100} and {010}. The calculated density based on the empirical formula is 3.268 g/cm^3. The mineral is optically biaxial (+), with α = 1.548(2), β = 1.556(3) and γ = 1.585(2) (measured at 590 nm). The $2V$ was not measured, calculated value is 56°. Birefringence is 0.037. No dispersion or pleochroism was observed. The optical orientation is $Z = \mathbf{c}$. Chemical analysis (EDS, 6 spots) is K_2O 7.93, MgO 3.11, CuO 0.79, SO_3 28.13, UO_3 48.94, H_2O (calc.) 12.53, total 101.43 wt. %, which yields the empirical formula $K_{1.94}(Mg_{0.89}Cu_{0.11})_{\Sigma1.00}(U_{0.99}O_2)_2(S_{1.01}O_4)_4(H_2O)_8$ (based on 28 O *apfu*). Prominent features in the Raman spectrum include the O–H stretching vibrations, symmetric stretching vibrations of $(UO_2)^{2+}$ ion, and stretching and bending vibrations of symmetrically non-equivalent SO_4 groups. The eight strongest powder X-ray diffraction lines are [d_{obs} Å ($I_{rel.}$) (hkl)]: 8.279(50)(010), 6.398(100)(200), 5.060(55)(210), 4.645(40)(012), 4.610(38)(211), 3.881(34)(021), 3.318(44)(221), 3.009(44)(213). The crystal structure of svornostite (R = 0.023 for 2745 reflections with $I_{obs} > 3\sigma[I]$) contains infinite uranyl sulfate chains of composition $[(UO_2)(SO_4)_2(H_2O)]^{2-}$ parallel to (001). The adjacent chains are linked through the Mg^{2+}-octahedra linked to the apical O atoms of the SO_4 groups with the chains and additionally by the K–O bonds and also H-bonds involving H_2O molecules. The uranyl sulfate chains are the same as found in the structures of several others uranyl sulfate minerals.

Keywords: svornostite, new mineral, uranyl sulfate, crystal structure, bond-valence, Jáchymov
Received: 10 February 2015; accepted: 24 March 2015; handling editor: F. Laufek
The online version of this article (doi: 10.3190/jgeosci.192) contains supplementary electronic material.

1. Introduction

Uranyl sulfates typically occur as supergene alteration products after hydration-oxidation weathering of uraninite (Plášil 2014). They are relatively common since uraninite is often associated with sulfides such as pyrite, marcasite or chalcopyrite (Finch and Murakami 1999; Krivovichev and Plášil 2013). Uranyl sulfates usually form during oxidizing weathering of sulfides and U ores in the old mining workings by the process connected to the acid mine drainage (AMD) (Fernandes et al. 1995; Brugger et al. 2003; Johnson 2003; Johnson and Hallberg 2005), generating highly mobile acid solutions containing dissolved UO_2^{2+}.

Svornostite is further new uranyl sulfate mineral found in Jáchymov (Joachimsthal), Czech Republic. The new mineral and the name were approved by the Commission for the new Minerals, Names and Classification of International Mineralogical Association (IMA2014-078). The new mineral was named after the type locality, abandoned Svornost mine (also known as *Einigkeit* in German). The holotype specimen is deposited in the collections of the

Fersman Mineralogical Museum of the Russian Academy of Sciences, Moscow, Russia, registration number 4537/1.

2. Occurrence

Svornostite was found on a single specimen collected from Geschieber vein on the 5th level of the Svornost mine, Jáchymov, Western Bohemia, Czech Republic by one of the authors (JH). The description of the locality and its geological setting has been already given in detail elsewhere (e.g., Ondruš et al. 1997, 2003; Tvrdý and Plášil 2010; Hloušek et al. 2014). The Jáchymov ore district is a classic example of the Variscan hydrothermal vein type of deposit, so-called five-elements formation, Ag–Bi–Co–Ni–(U). Jáchymov is the type locality for 43 minerals and more than 430 minerals have been identified from there.

Minerals found in direct spatial association with svornostite include geschieberite, $K_2(UO_2)(SO_4)_2{\cdot}2H_2O$ (IMA2014–006; Plášil et al. 2014a) and adolfpateraite (Plášil et al. 2012). Minerals are of supergene origin and formed during alteration during post-mining processes.

3. Physical and optical properties

Svornostite forms markedly elongated prisms (Fig. 1) in multiple intergrowths. Crystals, up to 0.2 mm across, are flattened on {100} and elongated parallel to [001]. It is light yellow in crystals and bright yellow in larger aggregates with a very pale yellow streak. Crystals are transparent to translucent (if thicker) with a vitreous luster. They are brittle, with a perfect cleavage on {100} and {010}, and uneven fracture. The Mohs hardness is estimated at 2. A density of 3.268 g/cm³ was calculated based on the unit-cell dimensions from single-crystal X-ray data and on the empirical formula from electron microprobe results. Svornostite shows strong yellowish-green fluorescence under both long- and short-wave UV radiation. The mineral is optically biaxial positive, with α = 1.548(2), β = 1.556(3) and γ = 1.585(2) (measured at 590 nm), birefringence of 0.037 and $2V_{\mathrm{calc.}}$ = 56°. No dispersion or pleochroism was observed. The optical orientation is Z = **c**. The Gladstone-Dale compatibility, $1 - (K_p/K_c)$, is good (0.039) for the empirical formula and the single-crystal unit-cell.

Tab. 1 Results of chemical analyses (in wt. %) of svornostite

	Mean (*n* = 6)	Range	SD	Standard
K_2O	7.93	7.34–8.71	0.48	Microcline
MgO	3.11	2.75–3.93	0.45	Olivine
CuO	0.79	0.00–2.40	1.23	Cu (metal.)
SO_3	28.13	25.44–30.70	2.51	$BaSO_4$ (synth.)
UO_3	48.94	44.99–51.72	2.74	UO_2 (synth.)
H_2O	12.53*			
Total	101.43			

* calculated from the structure
SD – standard deviation

4. Chemical composition

The chemical composition of svornostite was determined using a CamScan4D scanning electron microscope (SEM) equipped with an Oxford Link ISIS energy-dispersive X-ray spectrometer. An operating voltage of 20 kV was used with a beam current of 500 pA and a 1 µm beam diameter. The EDS mode on the SEM was chosen for the analysis instead of the WDS mode on the electron microprobe (EMP) because svornostite was found to be less stable under the high-vacuum and higher probe current. A special attention was paid to the overlap of the U and K lines in the EDS spectrum, thus to the good resolution of the KK_α and UM_α analytical lines during measurement of K; the U content was measured using the UL_α line. The content of molecular H_2O was not deter-

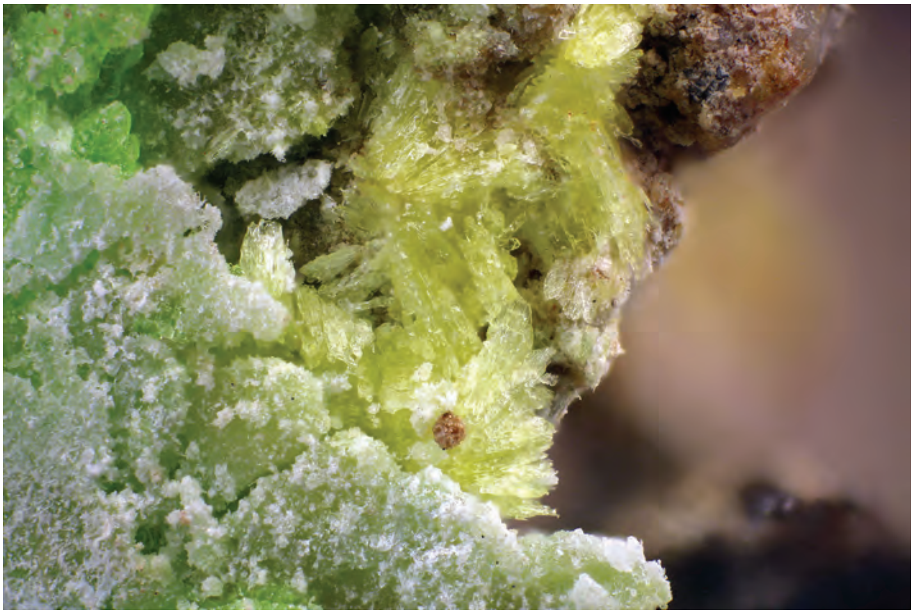

Fig. 1 Bright-yellow prismatic crystals of svornostite in association with greenish geschieberite (IMA2014-006) and coatings of white gypsum on altered gangue from Jáchymov. Width of image is 2.5 mm (photo P. Škácha).

mined directly, because of the paucity of pure material for thermal analysis. The H_2O content was calculated from stoichiometry obtained from the structure model. Presence of H_2O was independently proven by Raman spectroscopy.

The empirical formula of svornostite, calculated as the mean of 6 representative spot analyses (Tab. 1), is $K_{1.94}(Mg_{0.89}Cu_{0.11})_{\Sigma 1.00}(U_{0.99}O_2)_2(S_{1.01}O_4)_4(H_2O)_8$ (based on 28 O *apfu*). The simplified formula, $K_2Mg(UO_2)_2(SO_4)_4(H_2O)_8$, requires K_2O 8.05, MgO 3.43, UO_3 48.89, SO_3 27.32, H_2O 12.31, total 100 wt. %.

5. Raman spectroscopy

A Raman spectrum of svornostite (Fig. 2) was collected in the range 50–3500 cm^{-1} using a DXR dispersive Raman spectrometer (Thermo Scientific) mounted on a confocal Olympus microscope (100× objective). The Raman signal was excited by a 532 nm diode-pumped solid-state laser and detected by a CCD detector. The experimental parameters were: 5 s exposure time, 32 exposures, 400 lines/mm grating, 50 mm slit spectrograph aperture and 2.5 mW laser power level. The instrument was set up by a software-controlled calibration procedure using multiple neon emission lines (wavelength calibration), multiple polystyrene Raman bands (laser frequency calibration) and standardized white-light sources (intensity calibration).

The general features of the vibration spectra of uranyl-sulfate minerals and their characteristics were thoroughly reviewed by Čejka (1999). Recently, Raman spectra of several structurally related uranyl sulfates, among others bobcookite, $NaAl(UO_2)_2(SO_4)_4 \cdot 18H_2O$ (IMA2013-030, Kampf et al. 2014) were investigated. We based the assignment and interpretation of the Raman spectrum of svornostite on the similarities with the spectra of bobcookite and oppenheimerite, and also on the well-resolved Raman spectrum of natural zippeite (Plášil et al. 2010).

Interestingly, svornostite spectrum contains well-resolved O–H stretching vibrations, which is uncommon in case of unpolarized Raman spectroscopy. However, similarly well-resolved bands in the O–H stretching region were observed in the spectrum of bluelizardite (Plášil et al. 2014b) or plášilite (Kampf et al. 2015a). Raman bands at 3622, 3545 and 3496 cm^{-1} in the svornostite

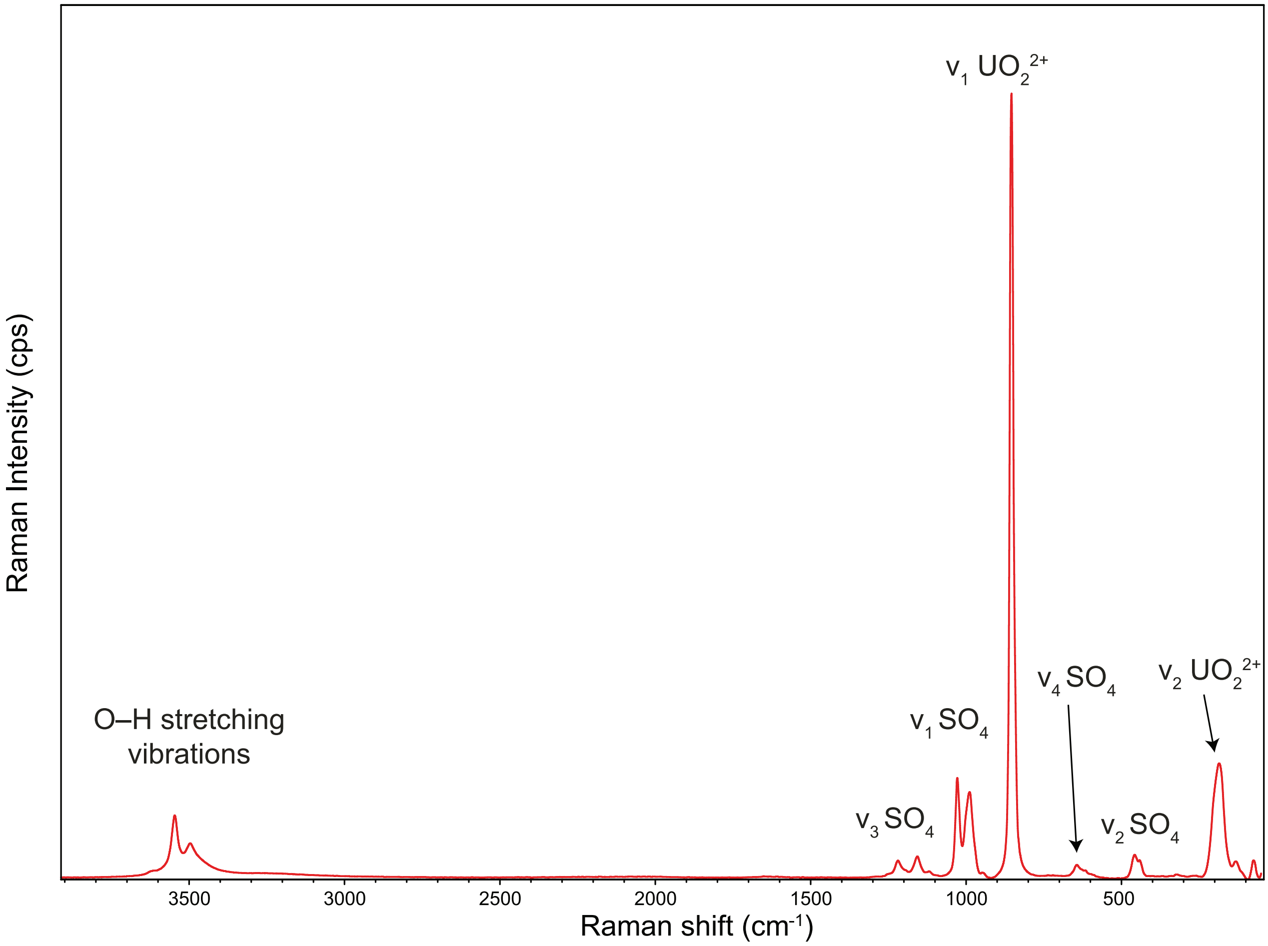

Fig. 2 The Raman spectrum of svornostite.

spectrum are attributed to υ O–H stretching vibrations of symmetrically distinct H_2O molecules. The O–H···O hydrogen bond lengths, inferred using the empirical relation given by Libowitzky (1999), vary in the range ~3.2 to 2.9 Å. These values are consistent with the O···O interatomic distances of the corresponding hydrogen- bonded H_2O molecules inferred from the X-ray structure study. Bands at 1220, 1200, 1155 and 1110 cm^{-1} are attributed to triply degenerate υ_3 $(SO_4)^{2-}$ antisymmetric stretching vibrations and those at 1028 and 989 cm^{-1} to υ_1 $(SO_4)^{2-}$ symmetric stretching vibrations. A very weak band at 951 and a very strong one at 854 cm^{-1} are assigned to υ_3 $(UO_2)^{2+}$ antisymmetric and υ_1 $(UO_2)^{2+}$ symmetric stretching vibrations, respectively. The approximate U–O bond length inferred from the respective wavenumbers of the $(UO_2)^{2+}$ vibrations after Bartlett and Cooney (1989) is ~1.76 Å, which is in line with the bond lengths obtained from the structure refinement. A very weak band at 725 cm^{-1} is probably connected with libration of H_2O molecules. Bands at 643 and 610 cm^{-1} are attributed to triply degenerate υ_4 (δ) $(SO_4)^{2-}$ bending vibrations, and those at 458 and 438 cm^{-1} to υ_2 (δ) $(SO_4)^{2-}$ bending vibrations. A weak band at 322 cm^{-1} can be assigned to the υ (U–O$_{\text{ligand}}$) vibration. A weak band at 268 cm^{-1} together with a shoulder at 207 cm^{-1} may probably be assigned to split, doubly degenerate υ_2 (δ) $(UO_2)^{2+}$ bending vibrations. However, the shoulder may be related to a set of lattice vibrations at 186, 132 and 75 cm^{-1}. From the number of observed bands of $(SO_4)^{2-}$ vibrations it may be inferred that structurally (symmetrically) distinct $(SO_4)^{2-}$ groups are present in the structure of svornostite.

6. X-ray crystallography and structure determination

6.1. Powder diffraction

X-ray powder diffraction data (Tab. 2) were obtained from a hand-picked sample using a PANalytical Empy-

Tab. 2 Powder diffraction data for svornostite

I_{rel}	d_{obs}	d_{calc}	I_{calc}	*h*	*k*	*l*
50	**8.279**	8.275	48	0	1	0
2	6.901	6.947	<1	1	1	0
32	6.661	6.660	27	0	1	1
100	**6.398**	6.393	100	2	0	0
20	5.613	5.611	18	0	0	2
55	**5.060**	5.059	52	2	1	0
40	**4.645**	4.644	40	0	1	2
38	**4.610**	4.612	37	2	1	1
1	4.359	4.365	2	1	1	2
23	4.217	4.217	24	2	0	2
5	4.137	4.137	3	0	2	0
2	3.983	3.985	2	3	0	1
34	**3.881**	3.882	35	0	2	1
29	3.757	3.757	30	2	1	2
7	3.588	3.590	2	3	1	1
24	3.409	3.409	27	0	1	3
6	3.330	3.330	5	0	2	2
44	**3.318**	3.318	49	2	2	1
6	3.218	3.222	1	1	2	2
22	3.197	3.197	27	4	0	0
44	**3.009**	3.008	50	2	1	3
4	2.986	2.982	7	4	1	0
14	2.955	2.953	15	2	2	2
5	2.884	2.882	8	4	1	1
6	2.800	2.806	8	0	0	4
19	2.776	2.775	17	0	2	3
4	2.758	2.758	1	0	3	0
16	2.679	2.679	17	0	3	1
10	2.658	2.657	10	0	1	4
5	2.634	2.633	10	4	1	2
3	2.602	2.601	1	1	1	4
6	2.570	2.569	8	2	0	4
11	2.546	2.545	13	2	2	3
5	2.533	2.533	5	2	3	0
5	2.476	2.475	5	0	3	2
15	2.470	2.470	11	2	3	1
10	2.467	2.468	10	4	2	1
6	2.454	2.454	6	2	1	4
1	2.431	2.430	<1	1	3	2
1	2.385	2.387	1	5	1	1
3	2.331	2.332	6	4	1	3
3	2.308	2.308	3	2	3	2
3	2.236	2.240	1	5	1	2
6	2.220	2.220	7	0	3	3
3	2.206	2.211	1	1	0	5
5	2.109	2.109	7	4	0	4
17	2.097	2.095	16	4	2	3
1	2.090	2.088	1	4	3	0
3	2.068	2.069	3	0	4	0
3	2.063	2.064	6	6	1	0
11	2.053	2.053	13	4	3	1
2	2.045	2.043	6	4	1	4
4	2.030	2.030	6	6	1	1
2	1.9938	1.9923	6	6	0	2
4	1.9736	1.9728	6	0	2	5
5	1.9678	1.9682	3	2	4	0
2	1.9569	1.9572	3	4	3	2
6	1.9408	1.9410	6	0	4	2
6	1.9358	1.9369	5	6	1	2
7	1.8861	1.8851	11	2	2	5
6	1.8704	1.8703	6	0	0	6
6	1.8667	1.8681	9	6	2	1
13	1.8574	1.8573	17	2	4	2

d values quoted in Å

rean diffractometer equipped with a PIXcel^{3D} detector using CuK_α radiation (45 kV, 40 mA) and operating in Debye-Scherrer geometry provided by focusing Göbel mirror optics. Data were collected in the range 3–50° 2θ, with the step size of 0.01° and counting time of 2 s per step, using an accumulation of 20 scans to improve the intensity statistics. Positions and intensities of diffractions were refined using a pseudo-Voigt shape function with the High-Score (PANalytical) program. Unit-cell parameters were refined by least-squares with the Celref program (Laugier and Bochu 2003). The theoretical pattern, used for indexing the experimental dataset, was calculated from the structure data using PowderCell (Kraus and Nolze 1996). Refined unit-cell parameters of svornostite obtained from powder data are a = 12.787(3), b = 8.275(2), c = 11.222(3) Å, with V = 1187.5(5) Å^3 and Z = 2.

Tab. 3 Crystallographic data and refinement details for svornostite

Crystal data	
Formula	$K_2Mg[(UO_2)(SO_4)_2]_2(H_2O)_8$
Crystal system	orthorhombic
Space group	$Pmn2_1$
Unit-cell parameters: a, b, c [Å]	12.7850(3), 8.2683(4), 11.2163(3)
Unit-cell volume [Å^3]	1185.68(7)
Z	2
Calculated density [g/cm^3]	3.280
Crystal size [mm]	0.235 × 0.068 × 0.052
Data collection	
Diffractometer	Oxford Diffraction Gemini with Atlas detector
Temperature [K]	300
Radiation, wavelength [Å]	MoK_α, 0.71073 (50 kV, 30 mA)
θ range for data collection [°]	2.9029.30
Limiting Miller indices	$h = -17 \rightarrow 16$, $k = -11 \rightarrow 11$, $l = -14 \rightarrow 14$
Axis, frame width (°), time per frame (s)	ω, 0.8, 350
Total reflections collected	19142
Unique reflections	3108
Unique observed reflections, criterion	2745, [$I > 3\sigma(I)$]
Absorption coefficient [mm^{-1}], type	14.492; multi-scan
T_{min}/T_{max}	0.574/1
R_{int}	0.047
F_{000}	1044
Structure refinement by Jana2006	Full-matrix least-squares on F^2
No. of ref. param., restraints, constraints	179, 1, 0
R, wR (obs)	0.0230, 0.0567
R, wR (all)	0.0280, 0.0587
GOF obs/all	1.38, 1.34
Weighting scheme, weights	σ, $w = 1/(\sigma^2(I)+0.0004I^2)$
Largest diff. peak and hole (e$^-$/Å^3)	–0.98, 1.40
Absolute structure parameter, Friedel pairs	0.018(9), 1410
Twin matrix	$\begin{pmatrix} -1 & 0 & 0 \\ 0 & -1 & 0 \\ 0 & 0 & -1 \end{pmatrix}$

6.2. Single-crystal X-ray diffraction and structure solution

A prismatic single crystal of svornostite, with dimensions 0.24 × 0.07 × 0.05 mm, was selected under the microscope and examined using an Oxford Diffraction Gemini single-crystal diffractometer with an Atlas CCD detector using monochromatized MoK_α radiation, with a fibre-optic Mo-Enhance collimator. The unit-cell dimensions were refined from 10483 reflections by least-squares with the CrysalisPro package (Agilent Technologies 2014). According to

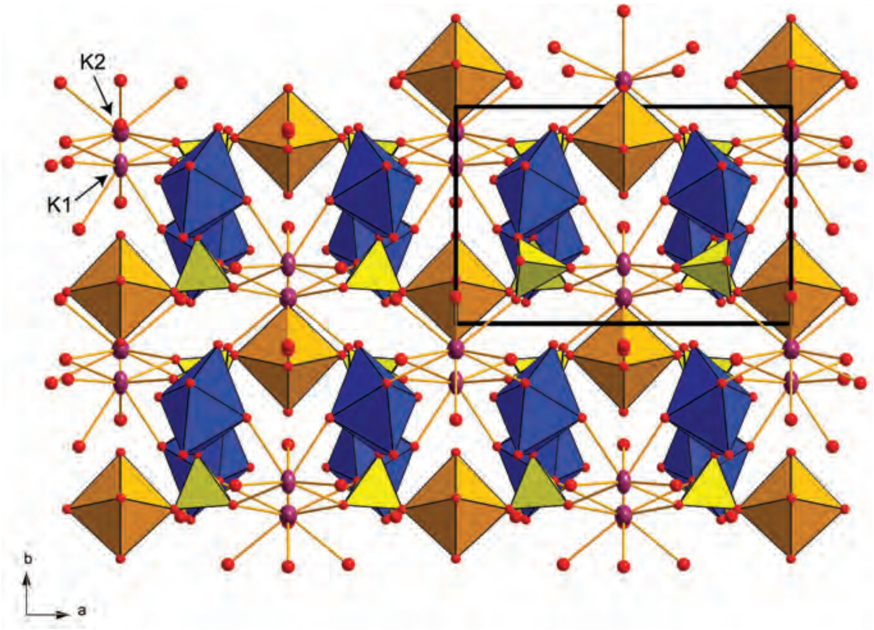

Fig. 3 The crystal structure of svornostite viewed down **c**. Infinite uranyl sulfate chains (blue and yellow, respectively) run parallel to the viewing direction. Adjacent chains are linked by Mg-octahedra (orange), the K–O bonds (K atoms are violet) and a H-bond network (not displayed); O atoms are red spheres. Unit-cell edges are outlined by the solid black line.

single-crystal X-ray data, svornostite is orthorhombic with a = 12.7850(3), b = 8.2683(4), c = 11.2163(3) Å, V = 1185.68(7) Å^3 and Z = 2. Of the 19142 collected reflections, 3108 were independent and 2745 were classified as observed based on the criterion [$I_{obs} > 3\sigma(I)$]. Data were corrected for Lorentz effect, polarization factor and background and an empirical (multi-scan) correction for absorption was applied to the dataset using the ABSPACK3 algorithm implemented in the RED routine of the CrysAlis software (Agilent Technologies 2014), leading to R_{int} of 0.047. Other details of the data collection are given in Tab. 3.

The crystal structure of svornostite was solved by the charge-flipping algorithm implemented in the Superflip program (Palatinus and Chapuis 2007) and subsequently refined using the software Jana2006 (Petříček et al. 2006, 2014) with the full-matrix least-squares refinement based on F^2. The reflection conditions and statistics indicated orthorhombic primitive cell and the non-centrosymmetric space group $Pnm2_1$ was confirmed by the refinement of the structure. Nearly all atoms with the unit-cell were found by the solution, some of the O atoms were localized by the difference Fourier syntheses. Nearly all atoms were refined using harmonic atomic-displacement parameters. Attempts to localize hydrogen atoms from the difference Fourier maps failed. The refinement converged smoothly with final indices of agreement R = 0.0230 and wR = 0.0567 for 2745 observed reflections with GOF = 1.34 (Tab. 3). The atom coordinates and the displacement parameters are given in Tab. 4 and selected interatomic distances in Tab. 5. Bond-valences are shown in Tab. 6.

6.3. Description of the crystal structure

The structure of svornostite (Fig. 3) contains one U, two S, one Mg, two K and eighteen O sites in the asymmetric unit. The U site, occupied by U^{6+}, is coordinated by 7 O atoms, two of which form the uranyl ion, UO$_2^{2+}$, and five more form a squat pentagonal bipyramid. This shares

Tab. 4 Atom coordinates and displacement parameters for the crystal structure of svornostite. The O10 atom refined isotropically.

Atom	x/a	y/b	z/c	U_{eq}/U_{iso}	U^{11}	U^{22}	U^{33}	U^{12}	U^{13}	U^{23}
U1	0.755069(14)	0.61283(2)	0.85798(4)	0.01161(6)	0.01420(11)	0.01179(11)	0.00883(10)	−0.00062(8)	0.00013(18)	0.0000(2)
K1	0.5	0.2719(3)	0.8707(3)	0.0351(7)	0.0217(11)	0.0133(11)	0.0118(10)	0.0014(7)	−0.0004(6)	−0.0003(8)
K2	1	0.8826(4)	1.0339(4)	0.0475(11)	0.0186(8)	0.0116(10)	0.0078(9)	−0.0008(8)	0.0003(8)	0.0000(7)
Mg	1	0.1579(4)	0.6665(3)	0.0288(11)	0.0203(10)	0.0527(14)	0.0323(14)	0	0	−0.0038(14)
S1	0.74623(12)	0.2420(3)	0.6685(2)	0.0156(6)	0.0288(16)	0.0395(19)	0.074(2)	0	0	0.0004(15)
S2	0.77026(15)	0.2595(3)	1.0488(2)	0.0127(5)	0.0248(19)	0.030(2)	0.0316(19)	0	0	0.0017(15)
O1	1	0.1964(12)	0.8516(10)	0.061(3)	0.023(4)	0.134(8)	0.027(4)	0	0	−0.020(7)
O2	0.6640(4)	0.1643(6)	0.7344(5)	0.0320(17)	0.029(3)	0.037(3)	0.031(3)	0.009(2)	0.016(2)	0.019(2)
O3	0.6577(4)	0.2552(6)	1.0454(5)	0.0274(16)	0.021(3)	0.034(3)	0.028(3)	−0.005(2)	−0.003(2)	0.009(2)
O4	0.8137(4)	0.3955(5)	0.9763(5)	0.0221(17)	0.024(3)	0.019(3)	0.024(3)	−0.002(2)	−0.001(2)	0.0127(19)
O5	0.8405(4)	0.1447(6)	0.6649(5)	0.0257(16)	0.019(3)	0.022(3)	0.036(3)	0.006(2)	0.002(2)	−0.005(2)
O6	0.8206(5)	0.1104(5)	1.0052(5)	0.0307(19)	0.038(4)	0.020(3)	0.035(3)	0.007(2)	−0.008(3)	−0.011(2)
O7	0.8086(4)	0.2879(6)	1.1735(4)	0.0230(15)	0.028(3)	0.027(3)	0.014(2)	0.006(2)	0.002(2)	−0.0063(19)
O8	0.7089(4)	0.9027(5)	0.8698(7)	0.0265(15)	0.045(3)	0.011(2)	0.024(3)	0.0012(18)	−0.006(3)	0.005(2)
O9	0.7065(4)	0.2736(6)	0.5468(4)	0.0216(15)	0.032(3)	0.026(3)	0.007(2)	0.001(2)	−0.002(2)	0.0019(18)
O10	1	0.9163(9)	0.6856(7)	0.0145(17)*						
O11	0.5	0.4422(10)	0.6289(7)	0.041(3)	0.032(5)	0.039(5)	0.052(5)	0	0	−0.003(4)
O12	0.8850(3)	0.6619(6)	0.8231(4)	0.0231(15)	0.015(2)	0.030(3)	0.024(3)	−0.004(2)	0.0044(17)	0.0032(18)
O13	0.6239(3)	0.5657(6)	0.8945(4)	0.0231(15)	0.017(2)	0.026(2)	0.027(3)	−0.004(2)	−0.0009(17)	0.0075(18)
O14	1	0.1207(16)	1.2173(10)	0.071(5)	0.076(10)	0.089(10)	0.046(7)	0	0	0.018(5)
O15	1	1.0993(12)	0.4828(9)	0.041(3)	0.012(4)	0.067(7)	0.043(6)	0	0	0.024(4)
O16	0.7725(5)	0.4015(7)	0.7218(6)	0.038(2)	0.064(5)	0.021(3)	0.028(3)	0.008(3)	−0.008(3)	−0.015(2)
O17	1	0.4055(8)	0.6389(6)	0.023(2)	0.010(3)	0.028(4)	0.030(4)	0	0	0.002(3)

* – refined with isotropic atomic displacement parameters

four of the equatorial vertices with sulfate tetrahedra such that each tetrahedron is linked to two uranyl bipyramids to form an infinite chain (Fig. 4). The free, non-linking equatorial vertex of the uranyl bipyramid is occupied by an H_2O molecule. The Mg site is coordinated octahedrally by six ligands including two O atoms and four H_2O molecules. The O atoms of the Mg octahedra belong to SO_4 tetrahedra of the chains. Therefore, Mg octahedra link adjacent chains (Fig. 3). Additional linkage is provided by the K–O bonds, involving either O atoms of the SO_4 groups or O_{Uranyl} atoms. Acceptors of the H–bonds (Tab. 6) within the structural units are the $O12_{Uranyl}$ atom, which can accept two H–bonds, the $O3_{Sulphur}$ atom, which can accept one H–bond, $O6_{Sulphur}$, which can accept two H–bonds and $O13_{Uranyl}$ and $O12_{Uranyl}$ atoms, which also can accept one H–bond. The structural formula of svornostite obtained from the refinement is $K_2Mg[(UO_2)(SO_4)_2(H_2O)]_2(H_2O)_6$. The EDS showed possibly Cu^{2+} to be entering most probably the octahedrally coordinated Mg site; however, this theory was not substantiated by the structure refinement.

Tab. 5 Selected interatomic distances (Å) and angles (°) in the structure of svornostite

U–O12	1.754(4)	S1–O2	1.436(6)	S2–O3	1.440(5)
U–O13	1.770(4)	S1–O5	1.449(5)	S2–O4	1.495(5)
U–O4	2.356(5)	S1–O9	1.480(5)	S2–O6	1.474(5)
U–O7^{i}	2.370(5)	S1–O16	1.486(6)	S2–O7	1.501(5)
U–O8	2.472(4)	<S1–O>	1.463	<S2–O>	1.478
U–O9^{ii}	2.368(5)				
U–O16	2.331(6)				
<U–O_{Ur}>	1.762				
<U–O_{eq}>	2.379				
K1–O2	2.743(6)	K2–O1^{v}	3.304(11)	Mg–O1	2.100(11)
K1–O2^{iii}	2.743(6)	K2–O2^{i}	3.099(6)	Mg–O5	2.042(5)
K1–O3	2.815(5)	K2–O6^{v}	2.985(6)	Mg–O5^{iv}	2.042(5)
K1–O3^{iii}	2.815(5)	K2–O9^{i}	2.943(5)	Mg–O10^{ix}	2.009(8)
K1–O11	3.056(9)	K2–O11^{i}	2.889(9)	Mg–O15^{ix}	2.117(10)
K1–O13	2.912(5)	K2–O12	3.329(5)	Mg–O17	2.070(7)
K1–O13^{iii}	2.912(5)	K2–O14^{ix}	2.847(13)	<Mg–O>	2.063
K1–O15^{ii}	3.317(10)	<K2–O>	3.057		
<K1–O>	2.914				
O1–O4	3.216(9)	O4–O9^{ii}	2.860(6)	O8–O9^{ii}	2.690(8)
O1–O4^{iv}	3.216(9)	O4–O11^{ii}	3.225(7)	O8–O12	3.050(7)
O1–O5	2.954(9)	O4–O12	2.939(6)	O8–O13	3.004(6)
O1–O5^{iv}	2.954(9)	O4–O13	2.952(7)	O8–O14^{i}	3.178(9)
O1–O6	2.955(9)	O4–O16	2.903(8)	O8–O15^{viii}	2.957(7)
O1–O6^{iv}	2.955(9)	O4–O18^{v}	2.851(3)	O9–O11	3.125(6)
O1–O10^{v}	2.971(13)	O5–O8^{i}	3.392(9)	O9–O12^{i}	2.819(6)
O1–O17	2.946(13)	O5–O9	2.413(7)	O9–O13^{i}	3.064(6)
O2–O5	2.392(7)	O5–O10^{v}	2.789(7)	O9–O16	2.384(8)
O2–O8^{v}	2.704(7)	O5–O15^{v}	2.910(9)	O10–O12	2.994(8)
O2–O9	2.354(7)	O5–O16	2.381(8)	O10–O12^{iv}	2.994(8)
O2–O11	3.329(8)	O5–O17	2.982(7)	O10–O15	2.732(12)
O2–O14^{vi}	3.160(11)	O6–O7	2.397(7)	O12–O12^{iv}	2.941(6)
O2–O16	2.406(8)	O6–O8^{v}	2.701(8)	O12–O16	2.828(8)
O3–O4	2.434(7)	O6–O9^{vii}	3.227(6)	O12–O17	3.305(7)
O3–O6	2.445(7)	O6–O14	3.305(10)	O13–O13^{iii}	3.167(6)
O3–O7	2.421(7)	O7–O8^{ii}	2.717(8)	O13–O15^{viii}	3.341(10)
O3–O10^{ii}	2.924(7)	O7–O11^{ii}	3.349(7)	O13–O16	3.034(8)
O3–O12^{ii}	3.235(7)	O7–O12^{ii}	3.019(6)	O13–O17^{ii}	3.175(7)
O3–O13	3.106(7)	O7–O13^{ii}	2.890(6)	O14–O15^{x}	2.984(15)
O4–O6	2.381(6)	O7–O14	2.853(8)	O15–O17^{ix}	3.078(12)
O4–O7	2.385(7)	O7–O16^{ii}	2.822(8)	O14–O15^{x}	2.984(15)

Symmetry codes: (i) $-x+3/2, -y+1, z-1/2$; (ii) $-x+3/2, -y+1, z+1/2$; (iii) $-x+1, y, z$; (iv) $-x+2, y, z$; (v) $x, y-1, z$; (vi) $-x+3/2, -y, z-1/2$; (vii) $-x+3/2, -y, z+1/2$; (viii) $-x+3/2, -y+2, z+1/2$; (ix) $x, y+1, z$; (x) $x, y-1, z+1$.

7. Discussion – structure topology and structure relations

The infinite uranyl sulfate chains present in the structure of svornostite are a well-known structural feature found in other uranyl sulfates, e.g., in bobcookite (IMA2014-030), $NaAl(UO_2)_2(SO_4)_4·18H_2O$ (Kampf et al. 2014), or the synthetic compounds $K_2[(UO_2)(SO_4)_2(H_2O)](H_2O)$ (Ling et al. 2010) and $Mn(UO_2)(SO_4)_2(H_2O)_5$ (Tabachenko et al. 1979).

It should be noticed here that svornostite is structurally very similar to the group of synthetic compounds prepared by Serezhkin and Serezhkina (1977, 1978, 1982) and by Tabachenko et al. (1979). These synthetic uranyl sulfate hydrates $M^{2+}[(UO_2)(SO_4)_2].xH_2O$ have layered structures ($x \sim 11$) or chain structures ($x \sim 5$); in all of them the $[(UO_2)(SO_4)_2(H_2O)]^{2-}$ units are present. The structural relations among these units were studied in detail especially in case of the Mg^{2+}-containing compounds. Uranium coordination polyhedra are pentagonal $[(UO_2)O_4(H_2O)]$ bipyramids. Each uranyl ion coordinates four monodentate sulfate groups and one water molecule as in svornostite. Layer structures ($x \sim 11H_2O$), where the $[M^{2+}(H_2O)_6]^{2+}$ octahedra and remaining water molecules are

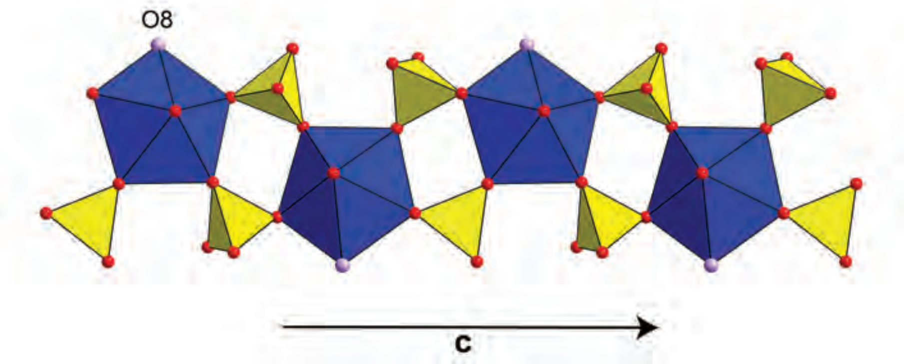

Fig. 4 Infinite uranyl sulfate chain found in the structure of svornostite; O8 marks the site occupied by H_2O.

Tab. 6 The bond-valence analysis for svornostite

	U	S1	S2	K1	K2	Mg	$\sum BV^A$	Species	$+H^+$
O1					0.04	0.33	0.37	H_2O	+1.6
O2		1.66		0.19×2↓	0.07×2↓		1.92	O	
O3			1.64	0.16×2↓			1.80	O	+0.2
O4	0.54		1.42				1.96	O	
O5		1.60				0.39×2↓	1.99	O	
O6			1.50		0.10×2↓		1.60	O	+0.4
O7	0.53		1.37				1.90	O	
O8	0.43						0.43	H_2O	+1.6
O9	0.53	1.48			0.11×2↓		2.12	O	
O10						0.43	0.43	H_2O	+1.6
O11				0.08	0.13		0.21	H_2O	+1.8
O12	1.77				0.04×2↓		1.81	O	+0.2
O13	1.71			0.12×2↓			1.83	O	+0.2
O14					0.14		0.14	H_2O	+1.8
O15				0.04		0.32	0.36	H_2O	+1.6
O16	0.57	1.45					2.02	O	
O17						0.36	0.36	H_2O	+1.6
$\sum BV^C$	6.08	6.19	5.93	1.06	0.95	2.22			

All values are in valence units (*vu*); ×2↓ – multiplicity; $\sum BV^C$ – sum of the bond-valences of cations; $\sum BV^A$ – sum of the bond-valences of anions; $+H^+$ – inferred contribution of the H-bonds; an average H-bond strength is of 0.2 *vu*, O_{donor}–H is equivalent to ~0.8 *vu* (Schindler and Hawthorne 2008). Values of +0.2 and +0.4 correspond thus to the acceptance of one or two H-bonds. A value of +1.6 is characteristic of the transformer H_2O group 2*0.8 *vu*. A value of +1.8 corresponds to the non-transformer H_2O group = Δ + 2*0.8 + 0.2 *vu*. Bond valence parameters are taken from Burns et al. (1997), for U^{6+}–O, and from Brown and Altermatt (1985) for K^+–O, S^{6+}–O and Mg^{2+}–O.

located between the layers, transform in chain structures (x ~ $5H_2O$) during the partial irreversible dehydration. During such dehydration process, all H_2O molecules non-coordinated to metal cations and the two H_2O molecules in *trans* positions of $[M^{2+}(H_2O)_6]^{2+}$ octahedra are released from the structure. In structures of pentahydrates, the coordination polyhedra involving M^{2+} consist of four H_2O and two terminal O atoms adhering to SO_4 groups, as in case of svornostite. Chemical formulae of both type of compounds are therefore $[Mg(H_2O)_6][(UO_2)(SO_4)_2(H_2O)].4H_2O$ and $[Mg(H_2O)_4[(UO_2)(SO_4)_2(H_2O)]$, respectively.

Acknowledgements. We appreciate kind cooperation of Pavel Škácha, who provided photomicrographs of svornostite. Professor V. N. Serezhkin (University of Samara) is highly acknowledged for e-prints of several papers of his. The current text benefited from the constructive comments of Nicolas Meisser and Stuart Mills. František Laufek is thanked for editorial handling of the manuscript. This research was financially supported by the post-doctoral grant of the GAČR no. 13-31276P to JP and by the long-term project DKRVO 2015-02 of the Ministry of Culture of the Czech Republic (National Museum 00023272) to J. Č.

Electronic supplementary material. Supplementary crystallographic data for this paper are available online at the Journal web site (*http://dx.doi.org/10.3190/jgeosci.192*).

References

Agilent Technologies (2014) CrysAlis CCD and CrysAlis RED. Oxford Diffraction Ltd, Yarnton, Oxfordshire, UK

Bartlett JR, Cooney RP (1989) On the determination of uranium–oxygen bond lengths in dioxouranium(VI) compounds by Raman spectroscopy. J Mol Struct 193: 295–300

Brown ID, Altermatt D (1985) Bond-valence parameters obtained from a systematic analysis of the inorganic crystal structure database. Acta Cryst B41: 244–248

Brugger J, Meisser N, Burns PC (2003) Contribution to the mineralogy of acid drainage of uranium minerals: marecottite and the zippeite-group. Amer Miner 88: 676–685

Burns PC, Ewing RC, Hawthorne, FC (1997) The crystal chemistry of hexavalent uranium: polyhedron geometries, bond-valence parameters, and polymerization of polyhedra. Canad Mineral 35: 1551–1570

Čejka J (1999) Infrared spectroscopy and thermal analysis of the uranyl minerals. In: Burns PC, Finch RJ (eds) Uranium: Mineralogy, Geochemistry and the Environment. Mineralogical Society of America and Geochemical Society Reviews in Mineralogy and Geochemistry 38, Washington, pp 521–622

Fernandes HM, Veiga LHS, Franklin MR, Prado VCS, Taddei JF (1995) Environmental impact assessment of uranium mining and milling facilities; a study case at the Poços de Caldas uranium mining and milling site, Brazil. In: Allan RJ, Salomons W (eds), Heavy Metal Aspects of Mining Pollution and Its Remediation. J Geochem Explor 52: 161–173

Finch RJ, Murakami T (1999) Systematics and paragenesis of uranium minerals. *In*: Burns PC, Finch RJ (eds) Uranium: Mineralogy, Geochemistry and the Environment. Mineralogical Society of America and Geochemical Society Reviews in Mineralogy and Geochemistry 38, Washington, pp 91–179

Hloušek J, Plášil J, Sejkora J, Škácha P (2014) News and new minerals from Jáchymov, Czech Republic (2003–2014). Bull mineral-petrolog odd Nár Muz (Praha) 22: 155–181

Johnson DB (2003) Chemical and microbiological characteristics of mineral spoils and drainage waters at abandoned coal and metal mines. Water Air Soil Pollut: Focus 3: 47– 66

Johnson DB, Hallberg KB (2005) Acid mine drainage remediation options: a review. Sci Total Environ 338: 3–14

Kampf AR, Plášil J, Kasatkin AV, Marty J (2014) Bobcookite, IMA2014-030. CNMNC Newsletter No. 21, August 2014, page 802. Mineral Mag 78: 797–804

Kampf AR, Kasatkin AV, Čejka J, Marty J (2015a) Plášilite, $Na(UO_2)(SO_4)(OH)\cdot 2H_2O$, a new uranyl sulfate mineral from the Blue Lizard mine, San Juan County, Utah, USA. J Geosci 60: 1–10

Kraus W, Nolze G (1996) POWDER CELL – a program for the representation and manipulation of crystal structures and calculation of the resulting X-ray powder patterns. J Appl Cryst 29: 301–303

Krivovichev SV, Plášil J (2013) Mineralogy and Crystallography of Uranium. In: Burns PC, Sigmon GE (eds) Uranium: From Cradle to Grave. Mineralogical Association of Canada Short Courses 43: pp 15–119

Laugier J, Bochu B (2003) CELREF: Unit Cell Refinement Program from Powder Diffraction Diagram. Laboratoires des Matériaux et du Génie Physique, Ecole Nationale Supérieure de Physique de Grenoble (INPG), Grenoble, France. Accessed on September 15, 2014, at *http://pcb4122.univ-lemans.fr/du-sdpd/nexus/ccp14/web/tutorial/lmgp/*

Libowitzky E (1999) Correlation of O–H stretching frequencies and O–H…O hydrogen bond lengths in minerals. Monatsh Chem 130: 1047–1059

Ling J, Sigmon GE, Ward M, Roback N, Burns PC (2010) Syntheses, structures, and IR spectroscopic characterization of new uranyl sulfate/selenate 1D-chain, 2D-sheet and 3D framework. Z Kristallogr 225: 230–239

Ondruš P, Veselovský F, Hloušek J, Skála R, Vavřín I, Frýda J, Čejka J, Gabašová A (1997) Secondary minerals of the Jáchymov (Joachimsthal) ore district. J Czech Geol Soc 42: 3–76

Ondruš P, Veselovský F, Gabašová A, Drábek M, Dobeš P, Malý K, Hloušek J, Sejkora J (2003) Ore-forming processes and mineral parageneses of the Jáchymov ore district. J Czech Geol Soc 48: 157–192

Palatinus L, Chapuis G (2007) Superflip – a computer program for the solution of crystal structures by charge flipping in arbitrary dimensions. J Appl Cryst 40: 451–456

Petříček V, Dušek M, Palatinus L (2006) Jana2006. The crystallographic computing system. Institute of Physics, Prague, Czech Republic. Accessed on March 24, 2015, at *http://jana.fzu.cz*

Petříček V, Dušek M., Palatinus L (2014) Crystallographic computing system Jana 2006: general features. Z Kristallogr 229: 345–352

Plášil J (2014) Oxidation–hydration weathering of uraninite: the current state-of-knowledge. J Geosci 59: 99–114

Plášil J, Buixaderas E, Čejka J, Sejkora J, Jehlička J, Novák M (2010) Raman spectroscopic study of the uranyl sulphate mineral zippeite: low wavenumber and U–O stretching regions. Anal Bioanal Chem 397:2703–2715

Plášil J, Hloušek J, Veselovský F, Fejfarová K, Dušek M, Škoda R, Novák M, Čejka J, Sejkora J, Ondruš P (2012) Adolfpateraite, $K(UO_2)(SO_4)(OH)(H_2O)$, a new uranyl sulphate mineral from Jáchymov, Czech Republic. Amer Miner 97: 447–454

Plášil J, Hloušek J, Kasatkin AV, Škoda R, Novák M, Čejka J (2014a) Geschieberite, IMA 2014-006. CNMNC Newsletter No. 20, June 2014, page 555. Mineral Mag 78: 549–558

Plášil J, Kampf AR, Kasatkin AV, Marty J (2014b) Bluelizardite, $Na_7(UO_2)(SO_4)_4Cl(H_2O)_2$, a new uranyl sulfate mineral from the Blue Lizard mine, San Juan County, Utah, USA. J Geosci 59: 145–158

Schindler M, Hawthorne FC (2008) The stereochemistry and chemical composition of interstitial complexes in uranyl–oxysalt minerals. Canad Mineral 46: 467–501

Serezhkin VN, Serezhkina LB (1977) New double uranyl sulfates. Radiokhim 19: 807–810 (in Russian)

Serezhkin VN, Serezhkina LB (1978) X-ray investigation of double uranyl sulfates $M\mathrm{UO_2(SO_4)_2.5H_2O}$. Zhur Neorgan Khim 23: 752–755 (in Russian)

Serezhkin VN, Serezhkina LB (1982) On some properties of disulfatouranylate hydrates of divalent metals. Zhur Neorgan Khim 27: 424–430 (in Russian)

Tabachenko VV, Serezhkin VI, Serezhkina LB, Kovba LM (1979) Crystal structure of manganese sulfatouranylate $MnUO_2(SO_4)_2(H_2O)_5$. Khoordinats Khim 5: 1563–1568 (in Russian)

Tvrdý J, Plášil J (2010) Jáchymov – Reiche Erzlagerstätte und Radonbad im böhmischen Westerzgebirge. Aufschluss 61: 277–292